Springer

Journal of Mechanical Science and Technology 22 (2008) 1475~1482

Journal of Mechanical Science and Technology

www.springerlink.com/content/1738-494x
DOI 10.1007/s12206-008-0424-7

Fuzzy logic versus a PID controller for position control of a muscle-like actuated arm

C. S. Lee[1,*] and R. V. Gonzalez[2]

[1]*Professor, College of Mechanical and Control Engineering, Handong Global University, Pohang, Korea*
[2]*Professor, Dept. of Mechanical Engineering, LeTourneau University, Longview, Texas*

(Manuscript Received October 15, 2007; Revised April 23, 2008; Accepted April 23, 2008)

Abstract

This study compares three different control algorithms for a muscle-like actuated arm developed to replicate motion in two degrees-of-freedom (df): elbow flexion/extension (f/e) and forearm pronation/supination (p/s). Electromyogram (EMG) is employed to help determine the control signal used to actuate the muscle cylinders. Three different types of control strategies were attempted. The first algorithm used fuzzy logic with EMG signals and position error as control inputs (Fuzzy Controller). The second algorithm incorporated moment arm information into the existing fuzzy logic controller (Fuzzy-MA Controller). The third algorithm was a conventional Proportional-Integral-Derivative (PID) controller, which operated solely on position and integration error (PID Controller). Overall, moment arm scaling aided the fuzzy logic control algorithm by improving movement accuracy as determined by relative error and correlation. The PID controller resulted in the most accurate movement tracking after fine tuning the control gains. This study implies that moment arm scaling is an effective tool for improving motion tracking accuracy of the fuzzy controller in the mechanical arm. The study also implies that PID controller can be used as a substitute for the fuzzy based controller once the desired motion is prescribed.

Keywords: Muscle-like actuated arm; EMG; Position control; Fuzzy control; PID control

1. Introduction

The human musculoskeletal system is complicated and highly redundant [1]. There exist more muscles than necessary to generate the joint moment and/or joint movement [2, 3]. Myoelectric signals that can be measured from muscle surfaces were used to control the upper extremity prostheses more than thirty years ago [4]. Trajectory and joint torques of a robot arm were estimated by using EMG signals and a neural network model [5]. A real-time virtual arm was developed and tested for studying neuromuscular control of arm movement [6]. We designed a mechanical arm according to the physiological alignment of muscles and attempted to control its position following the pre-recorded movement of an actual arm [7; Fig. 1]. EMG signals and conventional PID control logics are used to control the position of arm.

A mechanical arm, actuated by muscle-like elements, simulates motion in 4-df: elbow f/e, forearm p/s, wrist f/e, and wrist radial/ulnar deviation. Twelve air cylinders are used to represent twelve muscles[1] across the 4-df. EMG signals are employed to help determine the control signal used to actuate the cylinders. Due to the difficulty of representing muscle control through a direct interpretation of individual

*Corresponding author. Tel.: +82 54 260 1393, Fax.: +82 54 260 1312
E-mail address: cslee@handong.edu

1) Biceps Brachii (BIC), Brachialis (BRA), Brachioradialis (BRD), Triceps Brachii (TRI), Pronator Teres (PRT), Supinator (SUP), Extensor Carpi Radialis Longus (ECRL), Extensor Carpi Ulnaris (ECU), Extensor Digitorum Communis (EDC), Flexor Carpi Radialis (FCR), Flexor Carpi Ulnaris (FCU), Flexor Digitorum Superficialis (FDS).

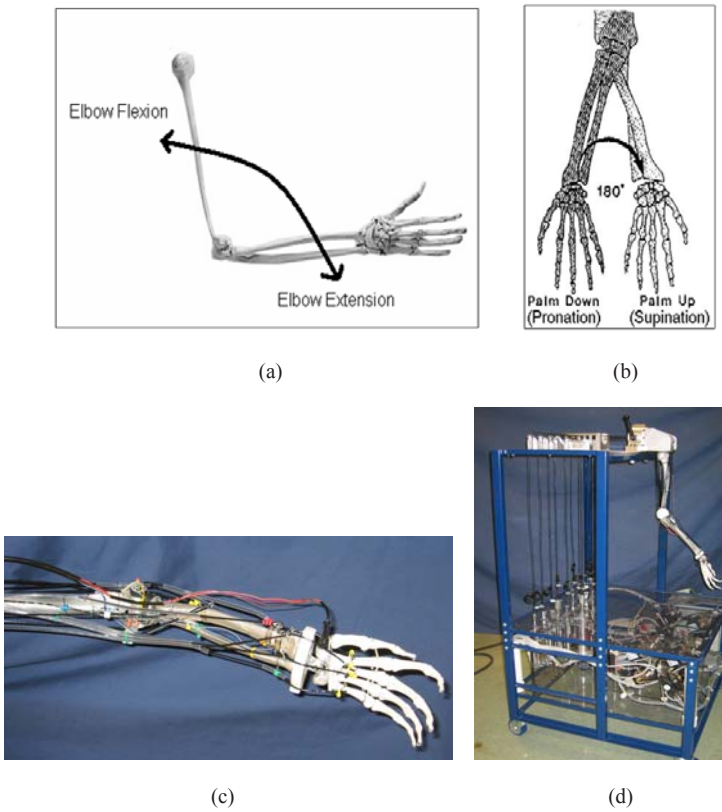

Fig. 1. Two degree of freedom elbow motion and a muscle-like actuated mechanical arm (a) Flexion/Extension (b) Pronation/Supination (c) Mechanical arm with 12muscles and 4-df including wrist motion (d) Experimental system.

muscle signals (EMG), a more robust controller for the arm was designed to simulate experimental arm movements. Three types of control algorithms were studied in 2-df at the elbow joint (f/e & p/s). Only seven actuators (simulated muscles) were used in control of the 2-df: BIC, BRA, BRD, ECRL, TRI, PRT, and SUP.

All controllers were implemented in LabVIEW™. The EMG signals, collected from human subjects, were rectified, low pass filtered, and scaled up to adjust to the same voltage levels of the valves that control the muscle cylinders. The arm controller takes these processed EMG signals and the desired position as inputs to help move the arm to the desired position. Inputs to the control algorithm were recorded from human subjects performing various 2-df elbow movements. A fuzzy logic control strategy was implemented due to the limited ability to acquire the complex mathematical relationships between individual muscle activity and arm movement. Thus, fuzzy logic implements intuitive rules into the algorithm by applying basic knowledge of motion control.

This research compared three different control strategies. The first strategy implemented fuzzy logic by using processed EMG signals and joint position as a means to develop an actuator control signal to reduce position error. Secondly, a moment arm scaling was incorporated into the fuzzy logic algorithm in an attempt to further reduce position error. Finally, a PID controller was implemented that did not consider individual muscle activity (EMG).

2. Methods

EMG signals and desired position were used as spreadsheet input to the controller programmed in LabVIEW™. An illustration of the experimental setup is shown in Fig. 2. F/e and p/s time-varying position of the arm was measured from two potentiometers and numerically compared with the desired position to produce position error. Using the EMG signals and position error, the controller determines the output voltage to each cylinder valve. A National Instruments Data Acquisition card (PCI-6033) was

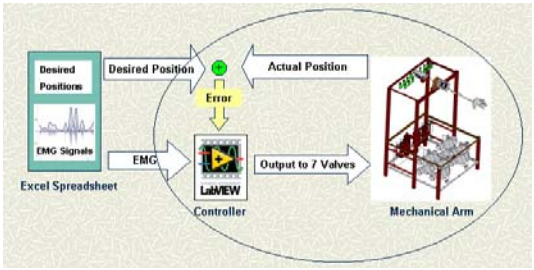

Fig. 2. Experimental setup. The controller determines output voltage to each valve that controls muscle cylinders by using processed EMG signals and position error.

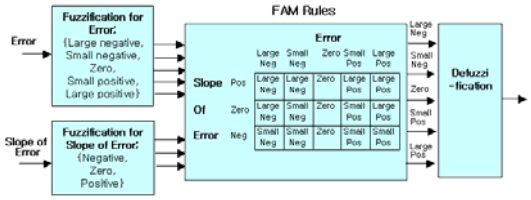

Fig. 3. Fuzzy control logic. Position error and slope error are fuzzified. FAM computes five outputs from the two sets of fuzzified variables using the Min-Max method. The five FAM outputs are multiplied by weight factors and summed. The deffuzzified output is added to the processed EMG signals and sent to a cylinder valve.

used to receive analog signals from the two potentiometers and convert them to digital values. A PCI-6703 was used to convert digital values to analog signals for actuating the cylinder valves. LABVIEW™ interfaces with these two cards and provides a helpful graphic user interface for observing control characteristics.

Position control using only the processed EMG signals as input resulted in inadequate control, making an advanced controller necessary. A fuzzy controller (Fuzzy) was developed which takes the processed EMG signals and modifies the signals by adding values determined by fuzzy logic. Fuzzy logic can be divided into three steps: fuzzification, fuzzy associated memory (FAM), and defuzzification (Fig. 3). The fuzzification step categorizes the position error into five fuzzy variables, and the slope error into three fuzzy variables. The position error was categorized into more variables because the controller was more sensitive to the position error than the slope error. The FAM computes five outputs from the two sets of fuzzified variables using the min-max method, a widely accepted way of implementing fuzzy variables [8, 9]. Rules for generating FAM outputs are constructed based on intuitive knowledge of motion control. For example, when the position error is 'large positive' and the slope error is 'negative', the FAM output is given as 'small positive'. Each muscle has its own unique FAM. In the defuzzification step, the five outputs from the FAM are multiplied by five weights and summed to produce a single output for each muscle. Output from the defuzzification process is added to the processed EMG signal and used to control the cylinder valves. The output was observed to fluctuate with time due to the discontinuous nature of the FAM rules, inherent in fuzzy control. To smooth the oscillatory nature of the output, a moving average method was implemented after defuzzification.

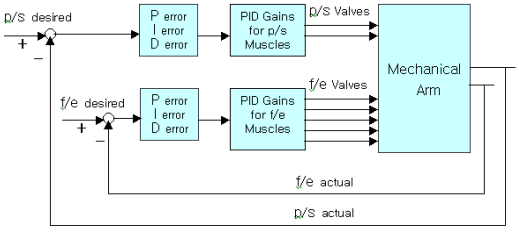

Fig. 4. Block diagram of PID controller. Voltage to each cylinder valve is obtained by summing P, I, and D errors multiplied by PID gains.

Another controller (Fuzzy-MA) that had moment arm information in the fuzzy control algorithm was developed. A moment arm is the quantification of the relationship between muscle force and joint torque. Hunt et al. [10] quantified moment arms vs. joint angles as polynomial regression coefficients for sixteen muscles in the human arm. Defuzzification weights were then varied based on the polynomial regression equations and the actual position of the arm to improve the accuracy and correlation of the controller. A larger defuzzification weight was used for a smaller moment arm to compensate for reduced mechanical advantage, whereas defuzzification weights were reduced for larger moment arms.

A PID controller (PID) was developed that did not use EMG signals. The PID control diagram is shown in Fig. 4. Desired values for f/e and p/s joint angles were compared with potentiometer measurements. Using the f/e and p/s errors, P, I, and D errors were calculated for each f/e and p/s angle and multiplied by PID gains for each muscle. The voltage obtained by summing the P, I, and D errors was sent to each cylinder valve of the mechanical arm. Eq. (1) was used

to calculate voltages for actuating f/e muscles and Eq. (2) for p/s muscles. If Eq. (1) was positive, the output voltage, V_i, was sent to the cylinder valves of each of the flexor muscles (BIC, BRA, BRD, and ECRL), and the extension muscle, TRI, was not activated. If Eq. (1) became negative, the voltage corresponding to the absolute value was supplied to the cylinder valve of the extension muscle and the four flexor muscles were not activated. The supinator muscle was actuated when Eq. (2) was positive, and the PRT was actuated when Eq. (2) was negative. For f/e muscles BIC, BRA, BRD, ECRL, and TRI (i=1,2,3,4,5):

$$V_i = K_{Pi} * FE_{Perror} + K_{Di} * FE_{Derror} + K_{Ii} * FE_{Ierror} \quad (1)$$

For p/s muscles PRT and SUP (i=6,7):

$$V_i = K_{Pi} * SP_{Perror} + K_{Di} * SP_{Derror} + K_{Ii} * SP_{Ierror} \quad (2)$$

Table 1 illustrates the coupling and redundancy of the seven muscles involved in f/e and p/s motions. As described previously, each muscle was attributed to one movement, as shown by X in Table 1. The PID controller did not allow antagonistic muscles to oppose each other as did the EMG driven fuzzy controller. There are an infinite number of possibilities for the twenty-one PID gains for the seven muscles. The configuration of PID gains was selected through trial and error. Initially, all the gains were set to 5.0. Then, they were changed intuitively in the direction that improved performance (explained in the next section). For f/e motion, K_p and K_i were set to equal values. For the p/s motion, K_i was set to zero, with a larger value for K_p. The gains for BRD and ECRL were set relatively small, since the primary flexor muscles were the BIC and BRA. The derivative gain, K_d, was set to zero for all the muscles, as it did not improve control results, but instead caused instability.

Table 1. Coupling and redundancy of seven muscles for f/e and p/s motions. X represents control action used for each muscle and O represents coupling involved in X motion of the muscle. PID gains obtained by trial and error are listed.

Muscle	Flexion	Extension	Pronation	Supination	Kp	Ki
BIC	X			O	5.0	5.0
BRA	X				5.0	5.0
BRD	X		O	O	2.5	2.5
ECRL	X	O		O	1.5	1.5
TRI		X			10.0	10.0
PRT	O		X		17.5	0.0
SUP	O			X	17.5	0.0

Three error analysis methods were used to quantify the performance of the controllers. The first, RMS error for each degree of freedom, estimates how far the actual is from the desired. The RMS error was calculated by using Eq. (3). If the desired and the actual are exactly the same, the RMS error is 0 and the correlation is 1.

$$\sqrt{\frac{\sum_{i=1}^{N}(desired_i - actual_i)^2}{\sum_{i=1}^{N}(desired_i)^2}} \quad (3)$$

The second method is the correlation factor between the actual and the desired positions for each degree of freedom and is calculated from Eq. (4). Upper bars represent mean values and σ represents standard deviation. The correlation factor represents how well the actual position follows the desired position. If they rise and fall together, the correlation is 1 and, if when one rises while the other falls, the correlation is -1.

$$\frac{\sum_{i=1}^{N}(desired_i - \overline{desired})(actual_i - \overline{actual})}{\sigma_{desired}\sigma_{actual}} \quad (4)$$

The third method, mean absolute error (MAE) between the actual and desired positions, is calculated from Eq. (5) for each degree of freedom.

$$\frac{\sum_{i=1}^{N}\left|desired_i - actual_i\right|}{N} \quad (5)$$

3. Results

Three different controllers were tested with all data included. No changes to the mechanical arm were allowed during testing after the arm was set to its initial position (mid pronated and fully extended) for each test. Twenty-two different sets of motion data, with ten distinct motions of f/e and p/s, were tested. The motions were designed with a combination of f/e and p/s movements. F/e movement ranged from a fully extended position to a 90º flexed position of the

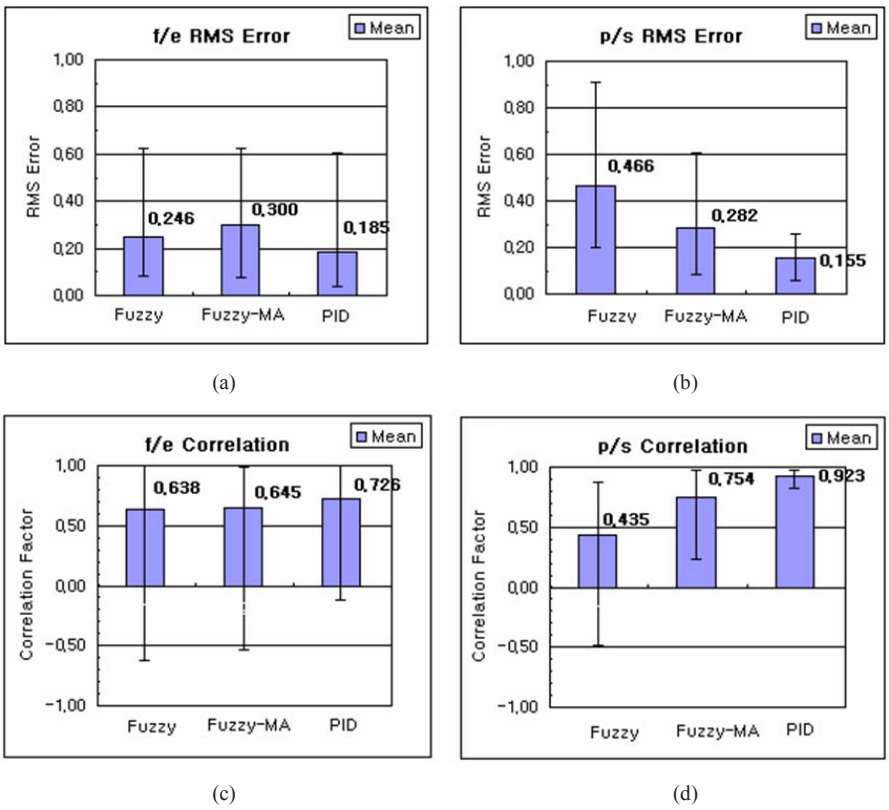

Fig. 5. Comparison of three controllers for RMS error and correlation factors. Bar charts represent mean values for twenty two motions and error bars represent maximum and minimum values. (a) f/e RMS error (b) p/s RMS error (c) f/e correlation (d) p/s correlation.

elbow. P/s motion ranged from a 90º pronation to a 90º supination. The motion lasted between 10 and 15 seconds.

Mean, minimum, and maximum values of RMS error and correlation factors for the twenty-two motion data are shown in Fig. 5 for the f/e and p/s motions. A p/s RMS error of 0.466 and a p/s correlation factor of 0.435 demonstrated poor performance for the p/s motion for the fuzzy controller. Improvement is observed in these values for the Fuzzy-MA. The p/s RMS error was reduced by 0.184, and the p/s correlation factor increased by 0.319. T-Test showed a significant improvement with p=0.004 for the p/s RMS error and p=0.003 for the p/s correlation factor. Significant improvement was not observed in the Fuzzy-MA controller for the f/e motion. F/e RMS error became larger, while the f/e correlation slightly increased.

The PID controller showed better performance than the Fuzzy-MA controller. F/e error was reduced by 0.115, and p/s error by 0.127. F/e correlation factor increased by 0.081, and p/s correlation increased by 0.169. Statistical analysis showed a significant improvement in the f/e RMS error (p=0.019), while it did not show much improvement in the f/e correlation (p=0.567). Significant improvements were achieved in both p/s RMS error (p=0.003) and p/s correlation factor (p=0.004).

Large values observed in the difference between the maximum and minimum values (MAX-MIN difference) of the RMS error and correlation factors indicate that the control performance was quite different depending on the desired motion. The three controllers showed similar values in the MAX-MIN difference of the f/e RMS error. However, the MAX-MIN difference of the f/e correlation factor decreased in the order of Fuzzy, Fuzzy-MA, and PID controllers. For the p/s motion, the Fuzzy-MA controller showed a considerable reduction in the MAX-MIN difference compared to the Fuzzy controller. Greater reduction was observed in the PID controller in comparison to the Fuzzy and Fuzzy-MA controllers. RMS error was

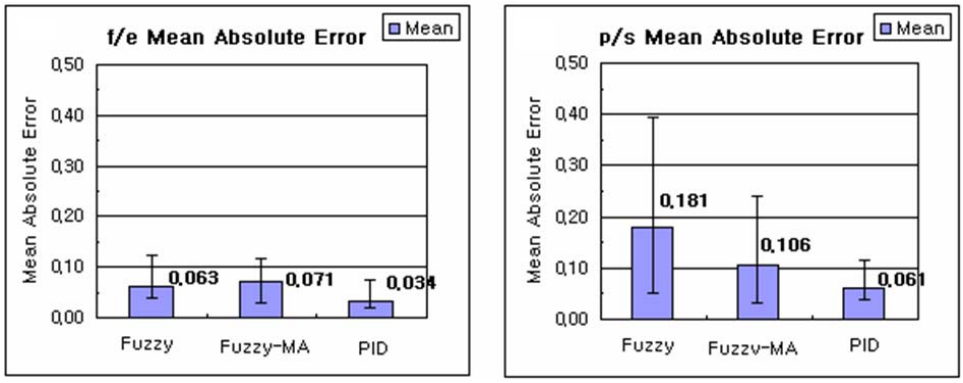

(a) (b)

Fig. 6. Comparison of three controllers for mean absolute error. Bar charts represent mean values for twenty two motions and error bars represent maximum and minimum values. (a) f/e mean absolute error (b) p/s mean absolute error.

observed to be larger in the f/e motion than the p/s motion for the Fuzzy-MA and PID controllers (Compare Fig. 5(a) and (b)). However, MAE error was much smaller in the f/e motion than the p/s motion, as shown in Fig. 6.

Moment arm information improved p/s motion control of the Fuzzy controller. Fig. 7 compares control graphs for the motion that slowly pronates, then supinates in the extended position of the arm. A normalized angle of 1.0 represents a fully supinated position of the elbow joint, and 0.0 represents a fully pronated position. It is apparent that the Fuzzy-MA controller helps pronation of the arm from the fully supinated position. The muscle voltage plot shows that the Fuzzy-MA controller supplies a voltage to the pronator valve as much as 2.5 times higher in comparison to the Fuzzy controller.

Better control results are clearly observed for the PID controller in the motion that slowly flexes and extends while pronated, as illustrated in Fig. 8. A normalized angle of 1.0 represents a fully extended position of the elbow joint, and 0.0 represents a fully flexed position of 90 degrees. The PID Controller quickly recovered from the initial position error, but the Fuzzy-MA controller could not recover this initial error. During the initial phase of the motion, the voltage to the BIC and BRA muscles (set to be equal) in the PID controller was observed to be close to one volt, while it was slightly below 0.5 volt for the Fuzzy-MA controller. During the f/e motion after the initial phase, the PID controller tended to follow the desired position with minimal error.

4. Discussion

The results indicated that using the moment arm information in the fuzzy controller noticeably improved p/s motion control. The muscle voltage plot indicated that the Fuzzy-MA controller supplies a voltage to the pronator valve several times higher in comparison to the fuzzy controller in the supinated position (see Fig. 7). This was possible since the Fuzzy-MA controller was programmed to have a larger defuzzification weight at the supinated angle of the arm. The larger weight was given to compensate for the reduced moment arm length at this joint angle.

Better control results were obtained in the PID controller compared to the fuzzy controllers. The PID Controller quickly recovered the position error that was initially present. The fuzzy controller and the Fuzzy-MA controller could not quickly recover this initial error (see Fig. 8). For the PID controller, this initial position error was accumulated by the integration error, and the corresponding muscles were activated until the error was reduced to zero. During the f/e and s/p motion after the initial phase, the PID controller tended to follow the desired position with minimal error, due to the dependency on feedback control action instead of EMG.

Pronation from the fully supinated position with the arm fully extended was easier for the PID controller than the Fuzzy-MA controller. Due to the proportional action of the PID controller, the arm started to strongly pronate as the p/s position error increased. The Fuzzy-MA controller also showed a strong pronator voltage at the moment when the arm began to

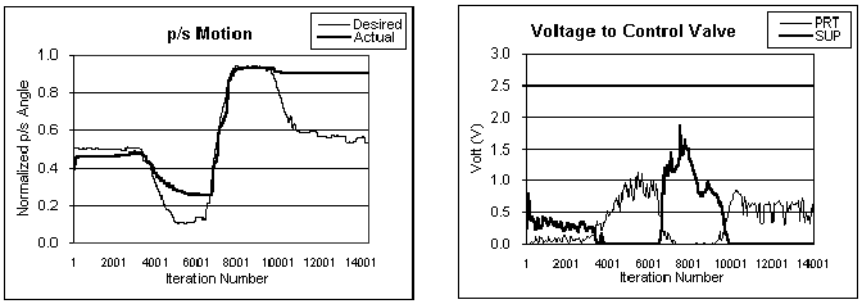

(a)

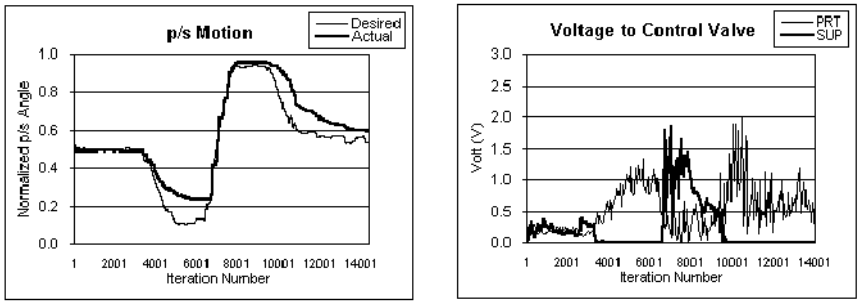

(b)

Fig. 7. Comparison of p/s motion and muscle control voltage for a motion that slowly pronates, then supinates in the extended position of the arm (a) Fuzzy controller (b) Fuzzy-MA controller.

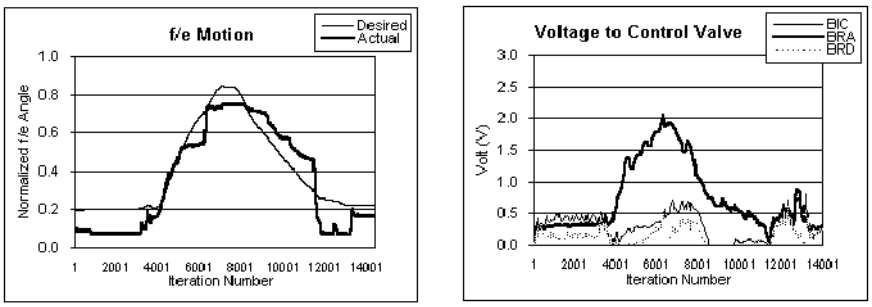

(a)

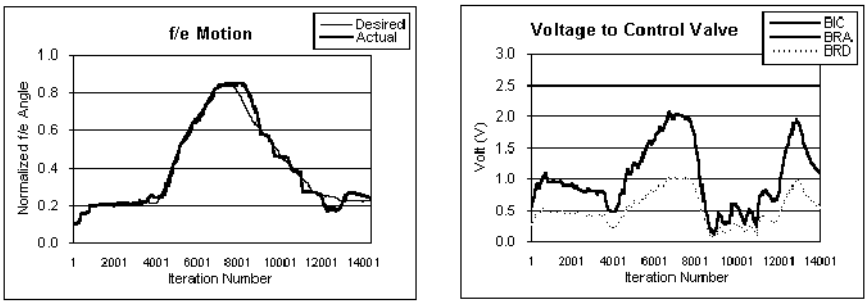

(b)

Fig. 8. Comparison of f/e motion and muscle control voltage for a motion that slowly flexes and extends while pronated (a) Fuzzy-MA controller (b) PID controller.

pronate from the fully supinated position, but the magnitude was smaller than the PID controller. Moreover, the voltage continued oscillating, which limited fast and strong pronation. The smaller RMS error and higher correlation factor in the p/s motion obtained with the PID controller are largely responsible for a strong and fast response with the PID controller at the fully supinated position with the arm fully extended.

As the denominator approaches zero, the RMS error, calculated by Eq. (3), becomes large. The correlation factor degrades as the motion remains unchanged. However, the MAE is not influenced by the type of motion because of the simple nature of the equation. For the Fuzzy-MA and PID controllers, the MAE was observed to be much smaller in f/e motion than p/s motion, which was an opposite trend compared to the RMS error and correlation. The opposite estimate is attributed to the presence of f/e motion close to zero during the entire period of motion for several motion data.

Motion and EMG data were collected at a sampling frequency of 960 Hz, resulting in test durations of 15 seconds for 14,396 points and 10 seconds for 9,596 points. However, the current mechanical arm showed a considerable delay before actuation due to static friction in the cylinders. This anomaly created a nonlinear mechanical response in the motion of the arm. In order to reduce the influence of hysteresis caused by the static friction, the run time was prolonged to fifty-two seconds by inserting delay routines in LabVIEW™. However, the mechanical arm exhibited a sudden change in motion at the moment when the static friction was overcome by the muscle force, which degraded control performance. The PID controller showed instantaneous fast motions when the error was large. The jerk was attributed to the force imbalance at the moment the static friction of the cylinder was overcome by the muscle force generated by the controller. Lower values in the PID gains were given to reduce such instantaneous fast motions, and consequently the control performance was compromised.

This study showed that moment arms incorporated into the fuzzy logic control improved the mechanical arm's response. The study demonstrated that a PID controller provides better accuracy than the EMG driven fuzzy based controllers.

Acknowledgment

This research was supported by NSF-BES Grant (RUI-0201889)

References

[1] M. Kent and D. G. Van, Human Anatomy, Brown Publisher, Dubuque, Iowa (1984).

[2] D. A. Winter, Biomechanics and motor control of human movement, Wiley, New York, (1990).

[3] B. M. Nigg, W. Herzog, Biomechanics of the musculo-skeletal system, Wiley, New York, (1999).

[4] R. Sorbye, Myoelectric controlled hand prostheses in children, *Int. J. Rehab. Res.*, 1 (1977) 15-25.

[5] Y. Koike, Y. and M. Kawato, Estimation of dynamic joint torques and trajectory formation from surface electromyography signals using a neural network model, *Biological Cybernetics*, 73 (1995) 291-300.

[6] K. Manal, R. V. Gonzalez, D. G. Lloyd and T. S. Buchanan, A real-time EMG-driven virtual arm, *Computers in Biology and Medicine*, 32 (2002) 25-36.

[7] S. Plymale, E. Landrum, D. Buchanan and D. Huizenga, Final Report for Senior Design Project of Biomedical Electrical Engineering Team, LeTourneau University, (2004).

[8] A. Kandel and G. Langholz, Fuzzy Control Systems, CRC Press, (1994).

[9] J. W. Hines, Fuzzy and Neural Applications in Engineering, John Wiley & Sons, (1997).

[10] B. V. Hunt and R. V. Gonzalez, Using Musculoskeletal Properties to Develop a Normalized Potential Moment Contribution Index for Individual Arm Muscles, *ASME National Congress*, Anaheim, CA, Nov, (2004).